Climate Dynamics (2005)
DOI 10.1007/s00382-005-0086-4

M. Barreiro · G. Philander · R. Pacanowski
A. Fedorov

Simulations of warm tropical conditions with application to middle Pliocene atmospheres

Received: 9 June 2005 / Accepted: 21 October 2005

Abstract During the early and mid-Pliocene, the period from 5 to 3 million years ago, approximately, the Earth is believed to have been significantly warmer than it is today, but the reasons for the higher temperatures are unclear. This paper explores the impact of recent findings that suggest that, at that time, cold surface waters were absent from the tropical and subtropical oceanic upwelling zones. El Niño was in effect a perennial rather than intermittent phenomenon, and sea surface temperatures in low latitudes were essentially independent of longitude. When these conditions are specified as the lower boundary condition for an atmospheric GCM, we find that the trade winds along the equator, and hence the Walker Circulation, collapse. The low-level stratus clouds in low latitudes diminish greatly, thus reducing the albedo of the Earth. The atmospheric concentration of water vapor increases, and enhanced latent heat release due to stronger evaporation warms up the tropical atmosphere, particularly between 40°S and 20°N. Moreover, teleconnection patterns from the Pacific induce a warming over North America that is enhanced by surface albedo feedback, a process that may have helped to maintain this region ice-free before 3 Ma. The results presented here indicate that the suggested absence of cold surface waters from the tropical and subtropical oceanic upwelling zones could have contributed significantly to the Pliocene warmth.

M. Barreiro (✉) · G. Philander
Atmospheric and Oceanic Sciences Program,
Princeton University, Princeton, NJ 08544-0710, USA
E-mail: barreiro@princeton.edu

R. Pacanowski
Geophysical Fluid Dynamics Laboratory,
NOAA, Princeton, NJ, USA

A. Fedorov
Department of Geology and Geophysics, Yale University,
New Haven, CT, USA

1 Introduction

Climatic conditions during the early–middle Pliocene, 5–3 million years ago (Ma), pose an interesting problem. The available data indicate that conditions at that time were both similar to and also very different from those of today. The main external factors that determine climate—the global geography and the atmospheric concentration of greenhouse gases, especially CO_2 (van der Burgh et al. 1993) —were essentially what they are today. However, estimates of sea surface temperature (SST) from foraminifers, ostracods and diatoms, as well as a 25 m higher sea level indicate that the global climate was much warmer than the present (e.g., Sloan et al. 1996; Dowsett et al. 1996). It was sufficiently warmer for continental glaciers to have been absent from the northern hemisphere (NH) (Zachos et al. 2001). What processes could have contributed to the warm conditions of 3 Ma?

The Pliocene Research, Interpretation and Synoptic Mapping (PRISM) (Dowsett et al. 1996), a project started by the US Geological Survey during the 90's and still ongoing, aims to document the surface conditions during the middle Pliocene. This data set and a subsequent version of higher resolution, PRISM2 (Dowsett et al. 1999), include sea level, land ice distribution, surface topography, vegetation distribution and 12-month climatologies of SST and sea ice. Of particular interest is the reconstructed SST, which is about 4–6°C warmer than the present-day SST in high latitudes. At low latitudes the reconstructed SST shows little or no change from today's values.

As a first step toward understanding the causes of Pliocene warmth, several modeling studies have taken the PRISM data sets, and imposed them as boundary conditions to atmospheric general circulation models (Sloan et al. 1996; Haywood et al. 2000). These studies established that the global mean surface temperature was about 2–4°C higher than the present, mainly due to

higher SST and changes in ice distribution. The next question is then, what processes maintained the high SST in high latitudes? One hypothesis is increased ocean heat transport by ocean gyres and/or the thermohaline circulation (Ravelo and Andreasen 2000; Raymo et al. 1996). This view has been challenged by Kim and Crowley (2000) who proposed that the increased thermohaline circulation was a response to and not the cause of Pliocene warming. More recently, Haywood and Valdes (2004) found no significant increase in ocean heat transport with respect to today in a coupled model simulation of the Pliocene.

There is large uncertainty in the values of CO_2 concentration during the Pliocene, but some investigators argue that they were no larger than today (van der Burg et al. 1993). Suppose that CO_2 concentrations were higher. Simulations of global warming because of higher CO_2 values indicate that temperatures should be higher, not only in the extratropics, but also in tropical regions. Such results are inconsistent with the reconstructed PRISM2 SST, as previously noted by, e.g., Haywood and Valdes (2004). Some authors have argued for a combination of increased ocean heat transport and CO_2 concentration to account for the observed SST pattern during the Pliocene (Crowley 1996; Raymo et al. 1996).

Recent complementary reconstructions of Pliocene SST, mostly from areas of upwelling in the tropical and subtropical oceans, show novel features in these regions. Apparently, cold surface waters were absent from those regions up to 3 Ma. Not only were the waters in the equatorial Pacific Ocean as warm in the east as the west (about 28–30°C; Cannariato and Ravelo 1997; Ravelo et al. 2004; Wara et al. 2005), but cold surface waters were also absent from the upwelling zones off the coasts of western South America (Haywood et al. 2005), southwest Africa (Marlow et al. 2000) and California (Ravelo et al. 2004; Haywood et al. 2005). Warmer waters also prevailed in the subtropical northeast Atlantic margin (Herbert and Shuffert 1998). Furthermore, Molnar and Cane (2002) have compared the global effects of El Niño in the present-day climate with the differences found in paleo-records between the middle Pliocene and today's climates. They concluded that an El Niño-like state characterized the climate up to 3 Ma.

The SST reconstructions agree on the state of the western tropical Pacific during early Pliocene. However, their differences are significant in the eastern side of the basin. The most likely reason for the discrepancy is the different localities used in PRISM2 and the new non-PRISM data, which does not allow for a direct comparison (Dowsett et al. 2005). PRISM2 has only one tropical point east of the dateline (Dowsett et al. 1999), away from the core of the present cold tongue. Hence the PRISM2 SST reconstruction in the eastern Pacific may not be representative of past conditions. On the other hand, the non-PRISM data includes localities from the core of the cold tongue and subtropical upwelling regions, and are likely to provide a better indicator of the east–west gradient during the Pliocene.

In the smaller tropical–subtropical Atlantic PRISM2 has a larger density of data. There, localities are close and both PRISM2 and non-PRISM data show a warmer-than-present SST off Namibia and Western Sahara. The reconstructions, however, differ in the amount of warming during the Pliocene, with the non-PRISM data showing warmer SSTs (Haywood et al. 2005). This may be due to different locations, or different proxy techniques used in the reconstruction. While PRISM2 SST estimates are based on planktic foraminifer assemblages (Dowsett et al. 1999), the non-PRISM data use other techniques that include oxygen isotopic composition (Ravelo et al. 2004), alkenone paleothermometry (Haywood et al. 2005; Marlow et al. 2000; Herbert and Shuffert 1998), and foraminiferal magnesium to calcium ratios (Wara et al. 2005). A description of the techniques and their shortcomings are beyond the scope of this work. Interested readers are referred to Haywood et al. (2005) who provide a very comprehensive comparison between PRISM2 and alkenone-derived data.

While different locations and proxy techniques may account for most of the differences between the above data sets, additional factors may also be important. A recent study using the same sites and technique as in Wara et al. (2005) suggests that the Pliocene warmth was not characterized by an El Niño-like state, but by a La Niña-like state (Rickaby and Halloran 2005). Thus, as proposed by Dowsett et al. (2005) and Haywood et al. (2005), multi-proxy temperature estimations at the same locations are needed in order to reduce uncertainties in reconstructed tropical SST. Such a multi-proxy approach has been carried out for sites describing the east–west SST gradient in the equatorial Pacific (Chaisson and Ravelo 2000; Ravelo et al. 2004; Wara et al. 2005), lending support to the findings of Wara et al. (2005) on the absence of the zonal gradient during the early Pliocene.

Theoretical studies can also contribute to a resolution of the controversy regarding tropical SST during the Pliocene by testing hypotheses concerning the causes of the warm conditions during the early Pliocene. Previous works have focused on the absence of northern glaciers, changes in ocean heat transport and higher concentrations of atmospheric CO_2, but the cause of Pliocene warmth is still unclear. What is the global impact of higher SSTs in low latitudes? In this paper we explore this hypothesis by assuming that SST patterns in low latitudes were essentially independent of longitude during the early Pliocene.

At present cold surface waters in the eastern equatorial Pacific contribute to intense easterly winds that advect moisture toward the western warm pool where convection is strong. The air thus rises in the western Pacific and tends to descend in the eastern side closing the so-called Walker circulation. This circulation is coupled to the surface ocean and maintains the east–west SST gradient that forces the winds. A second thermally driven tropical circulation, the Hadley cell, transport heat meridionally from its ascending branch in

the intertropical convergence zone (ITCZ) toward higher latitudes. The descending branches of the Walker and Hadley circulation maintain low-level stratus clouds in the eastern sides of the tropical oceans. These are boundary layer clouds that have a large albedo and that reflect a large portion (more than 30%) of the incoming solar radiation. The stratus clouds depend on the local vertical static stability, which in the deep tropics is mainly controlled by the SST because the temperature of air aloft is kept relatively constant by the large-scale atmospheric circulation. If the SST should increase in the cold regions then a positive feedback could come into play: the warmer waters will cause a decrease in the low-level cloud cover, allowing more solar radiation to reach the surface so that the SST increases further. Warmer SST will also tend to increase the atmospheric water vapor content. This greenhouse gas will trap more longwave radiation, warming the atmosphere further and enhancing the evaporation, another positive feedback.

These qualitative arguments indicate that tropical SST patterns can have a profound effect on the atmospheric circulation and hence the global climate. Yin and Battisti (2001) quantify this effect for the conditions of the Last Glacial Maximum, some 20,000 years ago. Here we investigate the role of tropical SST patterns in determining conditions during the early Pliocene.

In their observational study Molnar and Cane (2002) hypothesized that a permanent El Niño-like state would play a role in maintaining the Pliocene warmth, but do not test this idea further. More recently, Haywood and Valdes (2004) and Haywood et al. (2005) also suggested the possibility of a tropical control of climate during the Pliocene. They used a coupled ocean atmosphere general circulation model (GCM) with Pliocene conditions, and found that the simulated tropics becomes 1–5°C warmer than today. This result is consistent with the new non-PRISM paleo-records in that the tropical oceans warm—a feature not present in the PRISM2 data set. However, the simulated equatorial warming is uniform, thus maintaining the same east–west SST gradient of today. The authors note that changes in tropical SST, cloud cover, and the water vapor feedback might be important for tropical temperatures, and conclude that the dominant climate forcing during the Pliocene resulted from changes in the cryosphere and a strong positive feedback from clouds.

Philander and Fedorov (2003) hypothesized that the global cooling that led to the appearance of continental glaciers in high northern latitudes around 3 Ma ago also affected the thermal structure of the ocean by causing a gradual shoaling of the thermocline. When the thermocline became sufficiently shallow, the winds were able to bring cold water from below the thermocline to the surface in upwelling regions. This brought into play feedbacks involving ocean–atmosphere interactions of the type associated with ENSO and also mechanisms by which high-latitude surface conditions can influence the depth of the tropical thermocline. Because of the vast area of the tropics, any tropical changes could now affect the globally averaged surface temperature by influencing the Earth's cloud cover, albedo and concentration of the water vapor. Thus, as Philander and Fedorov argued, the transition from uniformly warm tropics to the tropics with zonal SST gradients (around 3 Ma) may have provided important positive feedbacks for the amplification of the glacial cycles.

In this modeling study we use an atmospheric GCM forced with idealized SST patterns to explore the role of the tropics in the climate of the early Pliocene. It complements previous atmospheric modeling studies by focusing specifically on the role of a tropical ocean state with zero east–west SST gradient on climate. We investigate the atmospheric circulation consistent with that state as well as the processes involved in warming the climate, and show that these ocean conditions could have contributed significantly to Pliocene warmth.

The manuscript is structured as follows. Section 2 provides a brief description of the atmospheric model and discusses the simulated atmospheric circulation consistent with the absence of cold surface waters in the tropics. Section 3 concentrates on the changes in the vertical structure of the tropical atmosphere and cloud distribution. Section 4 tests the robustness of the atmospheric response to Pliocene SST using different atmospheric GCMs. Section 5 compares the results of the Pliocene simulation with the atmospheric response to a surrogate of climate change and other SST patterns, and stresses the sensitivity of the atmosphere to imposed boundary conditions. The final Sect. 6 summarizes the results.

2 Tropical atmospheric circulation during mid-Pliocene

The atmospheric model used in this study is the Geophysical Fluid Dynamics Laboratory (GFDL 2005) Atmospheric Model 2 (AM2). A full description of the physical parameterizations of AM2 and a comparison of its simulation of the current climate with observations is provided in GAMDT (2005).

We hypothesize that the seasonal variations of SST along the dateline today represent the seasonal cycle at all longitudes in the tropical oceans during the early Pliocene. (Today the annual mean SST maximum is slightly south of the equator.) This new SST data set is hereafter called Tropical PLIOcene (TPLIO) and has the present seasonal variation of SST at the dateline between 40°S and 30°N, and has present conditions elsewhere. Linear interpolation is used for a smooth transition from the tropical to Polar regions (see Fig. 1). Sea ice is left at present values.

The purpose of these simulations is not to reproduce climatic conditions during the Pliocene, but to explore the role of the tropical SST on the atmospheric circulation at that time under the hypothesis of zero east–west tropical gradients. That is one reason for leaving SST in high latitudes unchanged, even though there is a

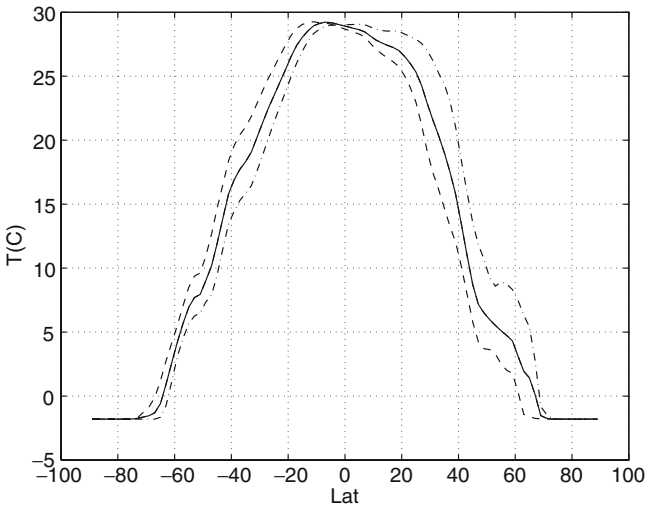

Fig. 1 SST at dateline: annual mean (*solid*), in March (*dashed*), in September (*dash-dot*)

consensus that during the Pliocene the extratropical oceans were significantly warmer than they are today. We note, however, that the tropical atmospheric circulation described below does not change significantly if the AM2 is forced with PRISM2 SST in the extratropics blended to TPLIO conditions in the tropics. The vegetation cover and continental configuration have also been left unchanged. The atmospheric concentration of CO_2 was kept at a value of 356 ppm in all experiments, close to the estimated value for the early Pliocene.

Pliocene topography was different from today's in certain regions (Thompson and Fleming 1996). The western cordillera of North America and northern South America were about half of today's elevations, and the East African Rift system is estimated to have been 500 m higher. Other areas with significant changes include Greenland due to the absence of ice sheets and Antarctica. Experiments with modified topography show that the tropical circulation changes presented here are largely insensitive to the American and African topography. In Sect. 5 the high latitude's topography is modified when addressing the influence of the NH ice cap in Pliocene climate.

The atmospheric circulation of AM2 forced with TPLIO is compared with a Control run in which the present climatologies of SST and sea ice are used as boundary conditions. Land ice is left at present values for both TPLIO and Control. We focus on the Pacific basin because of its largest importance in changing the global climate. Experiments were run for 11 years and the last 4 years were used to construct annual mean fields and seasonal cycles for analysis.

2.1 Winds

In the absence of east–west SST gradients in the tropics the surface trade winds in the equatorial region become very small, the Walker circulation disappears and upper-level westerlies are replaced by easterlies at all levels (Fig. 2). The Control run has only one region of wind

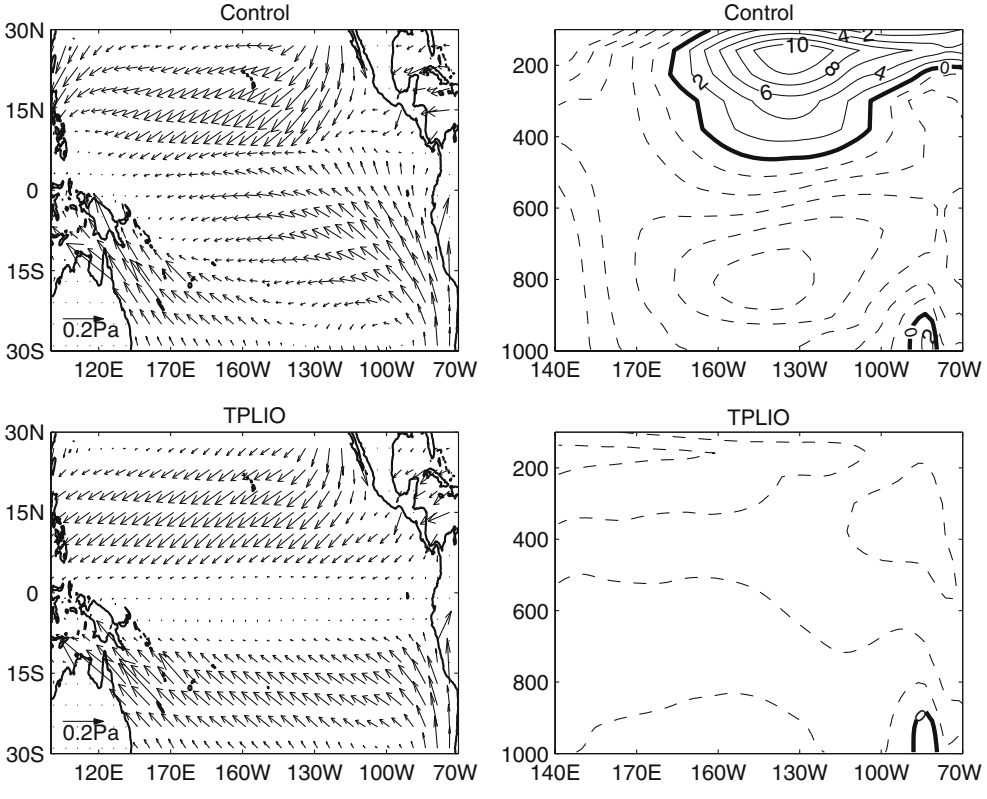

Fig. 2 Wind stress (Pa) and equatorial zonal winds (m/s) for Control (*upper panels*), and TPLIO (*lower panels*)

convergence over the tropical oceans marking the position of the ITCZ. In the absence of east–west SST gradient there are two regions of surface wind convergence, one north and the other south of the equator, which move seasonally accompanying the SST gradients (Fig. 3). The easterlies are weak between the two convergence zones, but stronger than Control south of 15°S (see also Fig. 4, left panel). Sensitivity experiments using different SST patterns demonstrate that the particular positions of the convergence regions depend on the latitudinal gradient of the imposed SST in agreement with previous studies (e.g., Hess et al. 1993).

The equatorial wind stress in TPLIO, averaged zonally over the whole globe, is about half the magnitude of that in the Control. At the same time, the southern (northern) hemisphere westerlies tend to strengthen (weaken) (Fig. 4). Significant changes are also seen in the annual mean meridional circulation of the atmosphere (Fig. 5). The northern branch of the Hadley cell is clearly stronger in TPLIO than in Control, while the southern branch tends to weaken. Also, the Hadley circulation is more equatorially symmetric due to the existence of a second ITCZ south of the equator in TPLIO. The existence of the second ITCZ creates a region of upward motion south of the equator and downward motion north of it. This increases the specific humidity in the atmospheric column between 0 and 30°S and decreases the water content in the northern tropics by weakening the northern ITCZ.

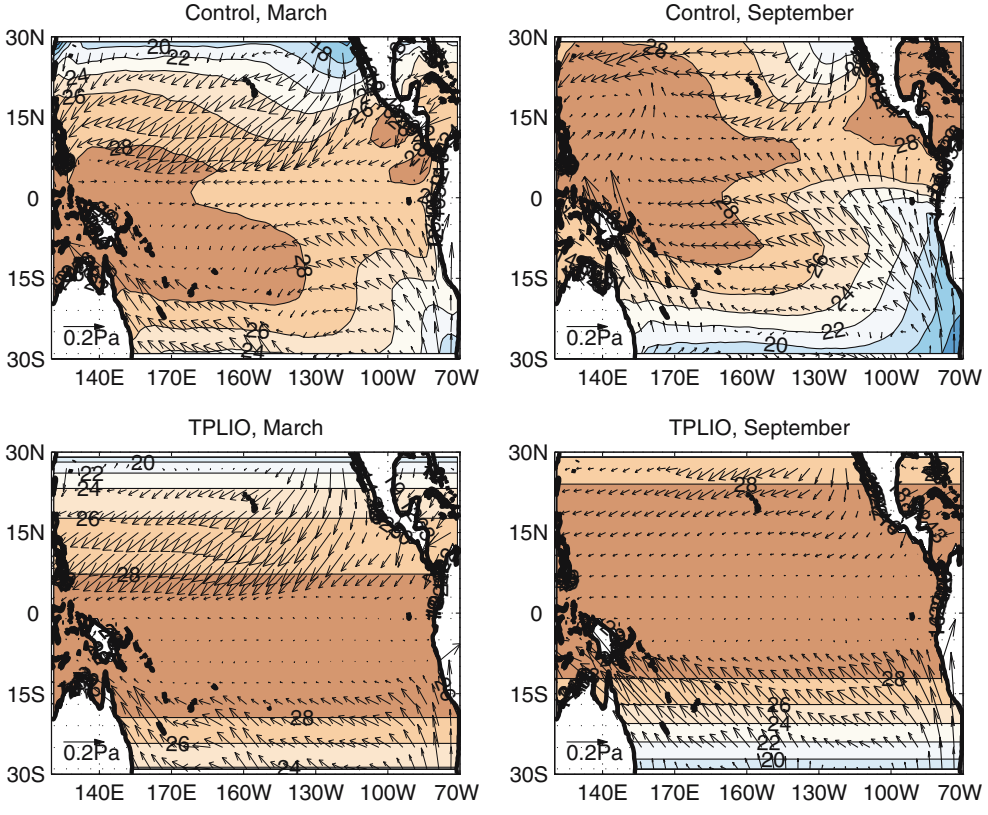

Fig. 3 Sea surface temperature and wind stress during March and September for Control (*upper panels*), and TPLIO (*lower panels*)

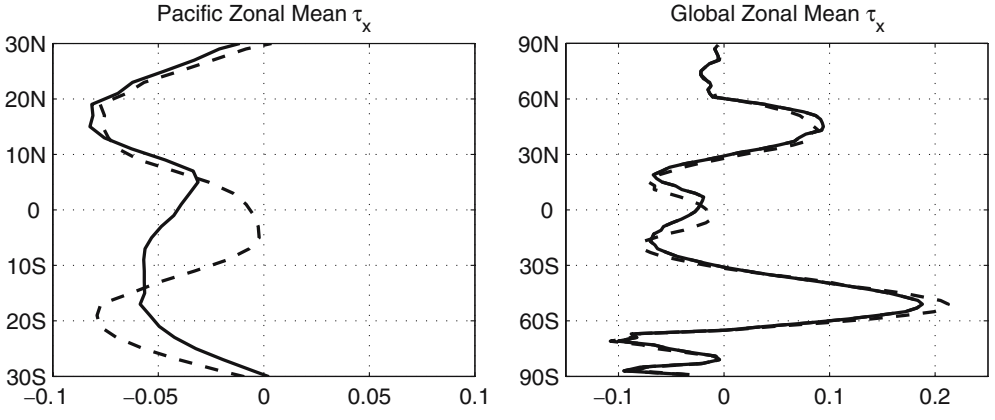

Fig. 4 Annual mean zonal wind stress (Pa) for Control (*solid*) and TPLIO (*dashed*): **a** zonal average over tropical Pacific only, **b** global zonal average

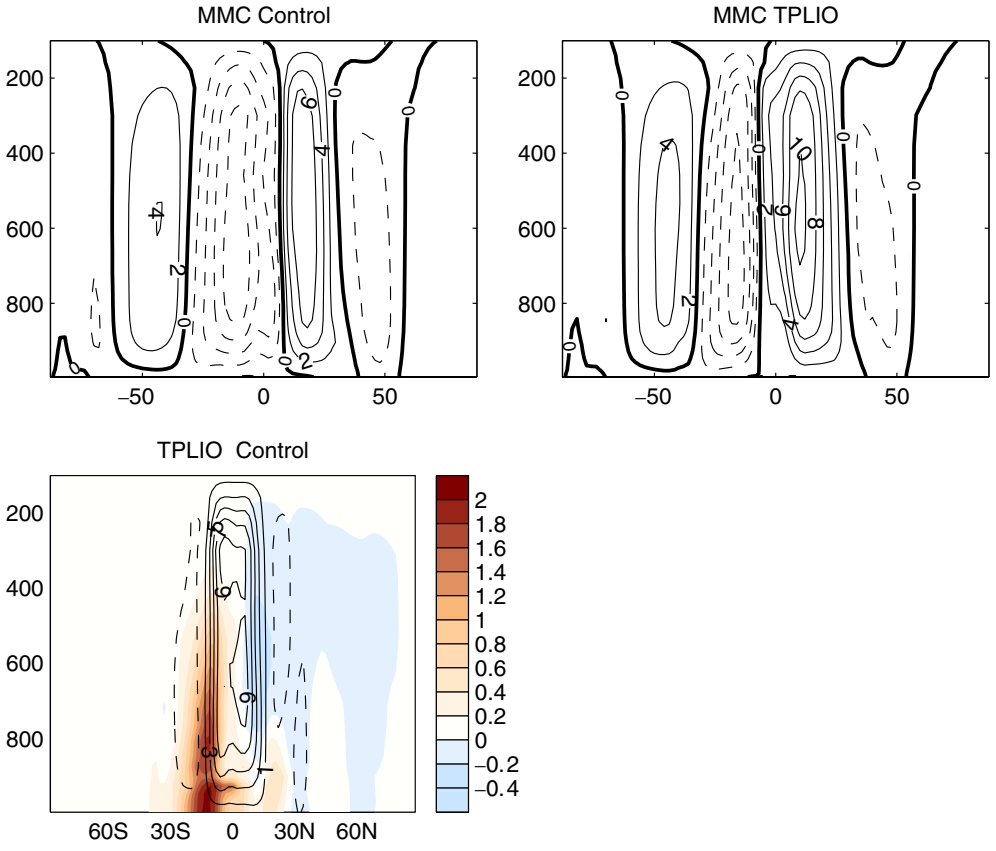

Fig. 5 Annual mean meridional circulation (1e10 kg/s) for Control (*upper left*), TPLIO (*upper right*) and the difference TPLIO–Control (*lower left*). Also shown is the difference in specific humidity between TPLIO and Control (10e-3 g/kg, *color shading*)

2.2 Precipitation and surface temperature

In the absence of a cold tongue, the surface wind convergence creates two ITCZs straddling the equator (Fig. 6). As mentioned in the previous section, the creation of a second ITCZ affects the structure and strength of the mean Hadley cell. This is particularly true in the eastern oceans. In the Control there is a well-defined region of upward motion denoting the location of the ITCZ in the eastern Pacific, and two regions of subsidence where the low-level stratus clouds develop. This picture has changed significantly in TPLIO, where two regions of ascending motion exist and the regions of subsidence have shrunken significantly.

The second ITCZ south of the equator causes the ocean to gain more freshwater in the eastern Pacific, a region currently dominated by evaporation. The western warm pool, on the other hand, becomes saltier due to decreased convection there. The Atlantic basin, in contrast to the Pacific, has a single ITCZ which is located to the south of the equator. These changes freshen the southern tropics and make the northern tropics saltier (Fig. 6, lower panel).

The global mean surface air temperature increase in TPLIO with respect to Control is 0.5°C. Figure 7 shows the spatial changes in surface air temperature and precipitation in TPLIO for NH winter and summer. Although this simulation includes neither altered SST patterns in high latitudes, nor the reduced extent of glaciers, the results are in general agreement with those of Molnar and Cane (2002) (hereafter MC) concerning the impact of permanent El Niño conditions.

For example, the simulation suggests that the area next to the Gulf of Mexico and the Caribbean was colder and wetter, while the high latitudes of North America were warmer than today. As pointed out by MC this pattern is consistent with paleo-records and are caused by teleconnections from the tropical Pacific. This is consistent with the map of sea-level pressure difference between TPLIO and Control, which describes a deeper and southward shifted Aleutian low. As a result warm air flows from the tropical north Pacific (Fig. 8) into higher latitudes of North America. The simulation also indicates a significant reduction in the surface albedo by about 30% due to changes in snow cover (Fig. 8). This suggests that the initial warming caused by atmospheric teleconnections is further enhanced by the surface albedo feedback. This process tends to move the freezing line (−2°C isotherm) northward, and may have been crucial in preventing North America from developing glaciers earlier than 3 Ma (Zachos et al. 2001).

The simulation also suggests that up to 3 Ma northern South America was drier, and eastern equatorial Africa wetter than today, in agreement with paleo-data (MC). In our simulations, changes are attributable not only to a permanent El Niño in the Pacific, but also to higher SST in the tropical Atlantic and Indian oceans. Thus, our results are somewhat different from MC. For

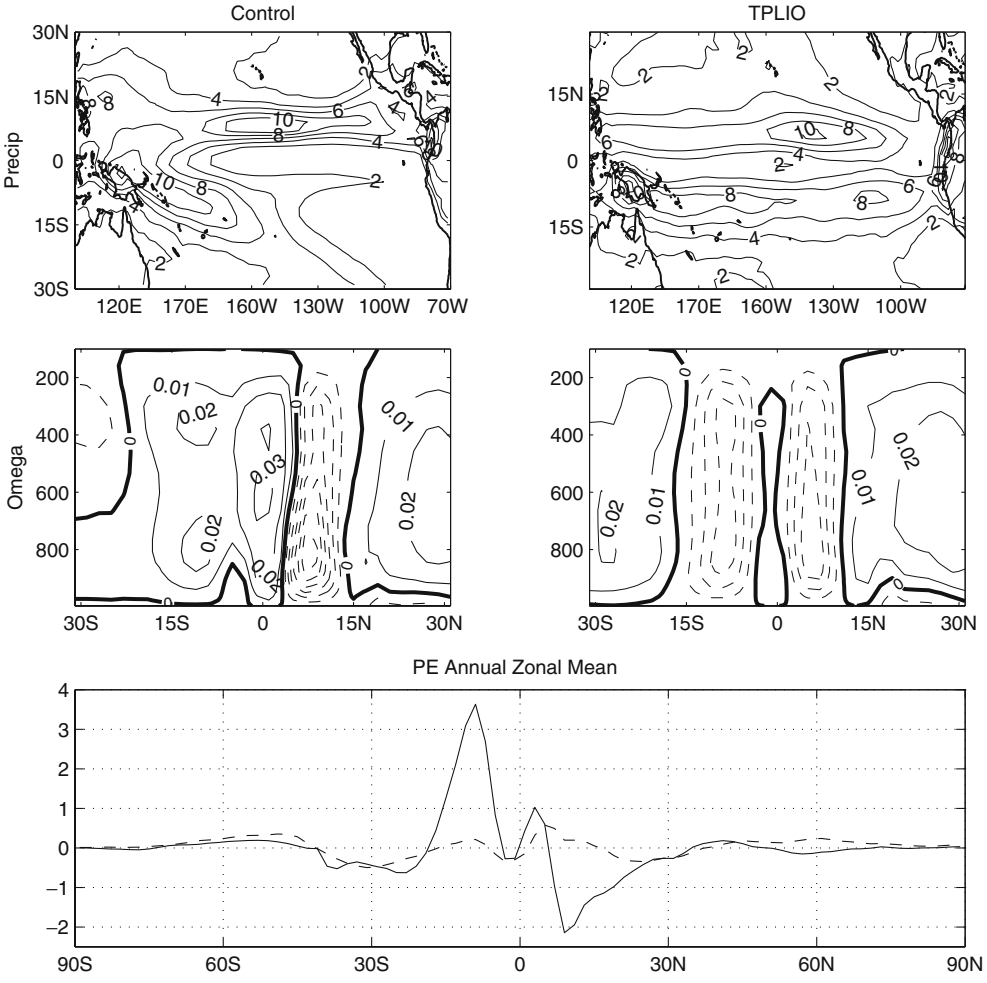

Fig. 6 Annual mean precipitation (mm/day) and vertical velocity in the eastern Pacific (Pa/s) for Control (*upper left panels*) and TPLIO (*upper right panels*). *Lower panel* annual zonal mean deviations with respect to Control of freshwater flux into the ocean for TPLIO (*solid*) and UNIF2K (*dashed*, see Sect. 5)

instance, MC note that El Niño should bring drier conditions to northern India and Australia, while there is evidence that they were wetter during the middle Pliocene. In our simulations Australia is wetter. Northeastern India shows a tendency for drier conditions, but there is a large wet anomaly in the northwestern region. This points out that the SST pattern throughout the tropics, not only that of the Pacific, influences climate patterns.

In TPLIO the southward shift of the ITCZ in the Atlantic brought heavy rains to Northeastern Brazil while the coasts of Ecuador and Peru received large amounts of rain because of the second ITCZ south of the equator in the Pacific.

2.3 Surface heat fluxes

The net downward surface heat fluxes in Control and TPLIO, and their difference are shown in Fig. 9 for the Pacific basin. Surface radiation and evaporation dominate the balance. The absence of east–west SST gradients reduces stratus cloud cover (see next section) and increases the net radiative flux into the ocean in the eastern Pacific. This positive feedback between SST and radiation is opposed and canceled by increased evaporation (due to changes in specific humidity) so that the ocean gains less heat in TPLIO than in the Control experiment in the eastern Pacific. The increased evaporation also creates a huge negative heat flux off Peru, which tends to cool the ocean significantly. In the central Pacific there is decreased evaporation due to the weakening of the trades, and the ocean gains more heat. As result, the net downward flux into the ocean is almost uniform along the equatorial region. In the tropical Atlantic changes are analogous to the Pacific, although they are not nearly as large because the present cold tongue is much weaker. In the Indian ocean decreased winds reduce evaporation and increase the flux of heat into the ocean in the Bay of Bengal and Arabian Sea.

3 Vertical temperature and cloud changes

To understand the changes in the tropical region, we can consider the simplified picture of an atmosphere in radiative–convective equilibrium. This atmosphere responds to SST changes by adjusting the vertical temperature profile in order to maintain a moist-adiabatic lapse rate (Soden 2000). Also, it is important to note that

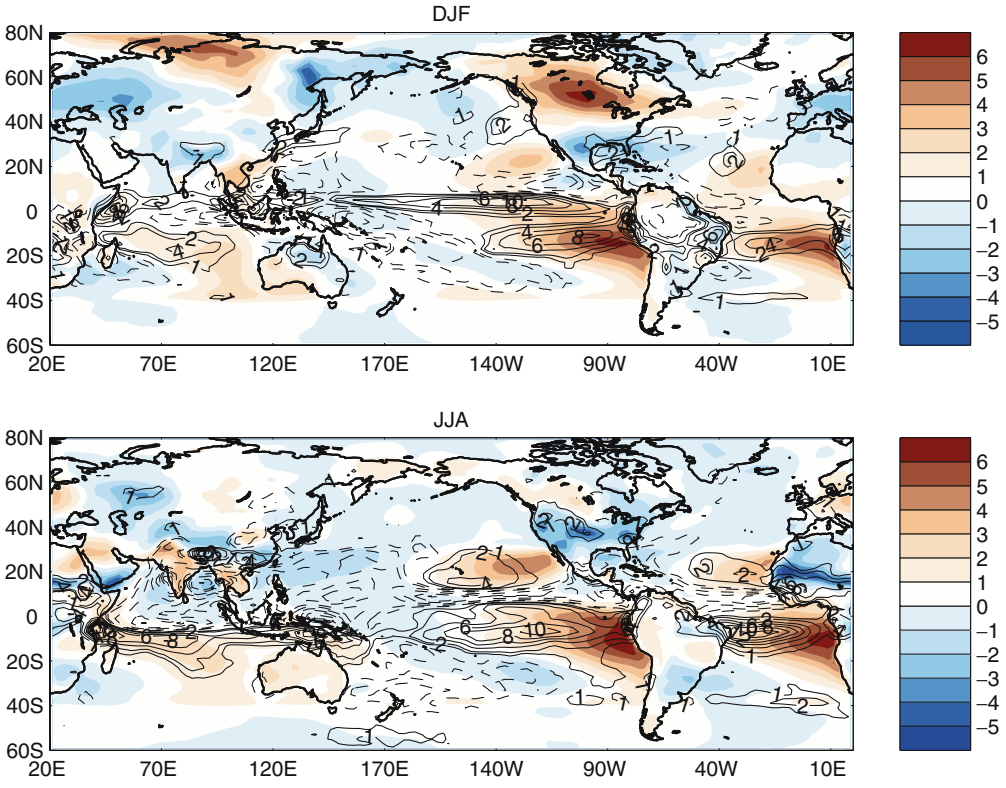

Fig. 7 Surface air temperature (*shading*) and precipitation (*contours*) differences between TPLIO and Control for December–February (*upper panel*) and June–August (*lower panel*). Precipitation in mm/day and temperature in degrees C

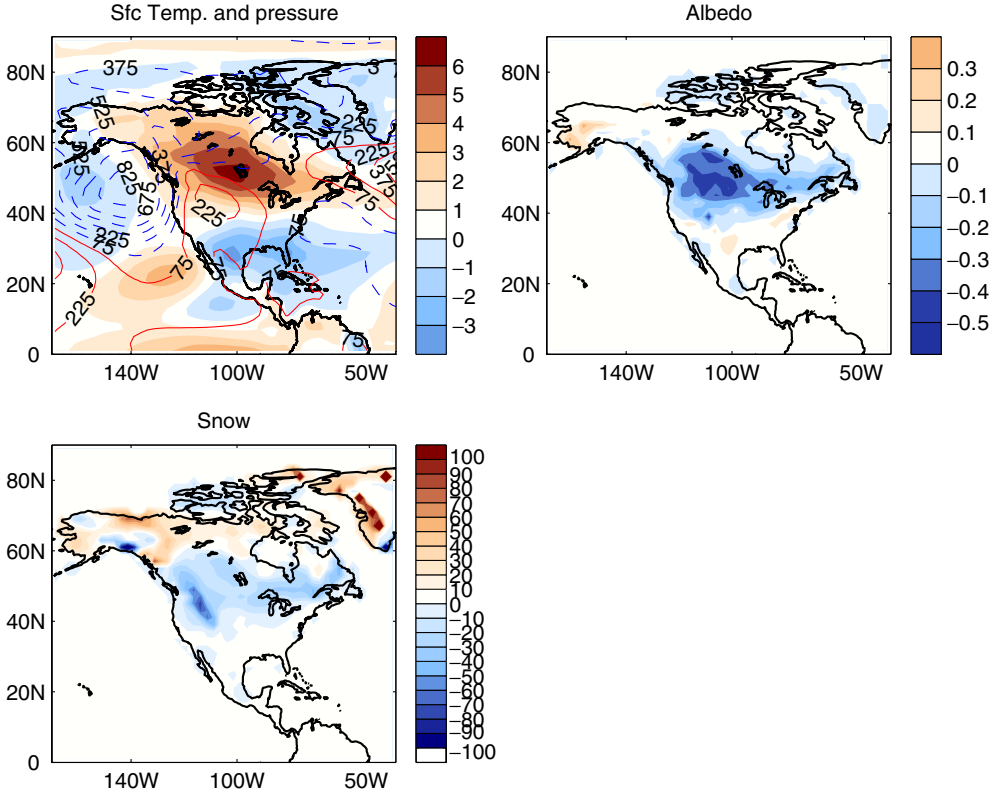

Fig. 8 Difference between TPLIO and Control experiments over North America. Surface air temperature (C) and surface pressure (Pa) (*upper left panel*), albedo fractional change (*upper right panel*), and snow difference (kg/m2, *lower left panel*)

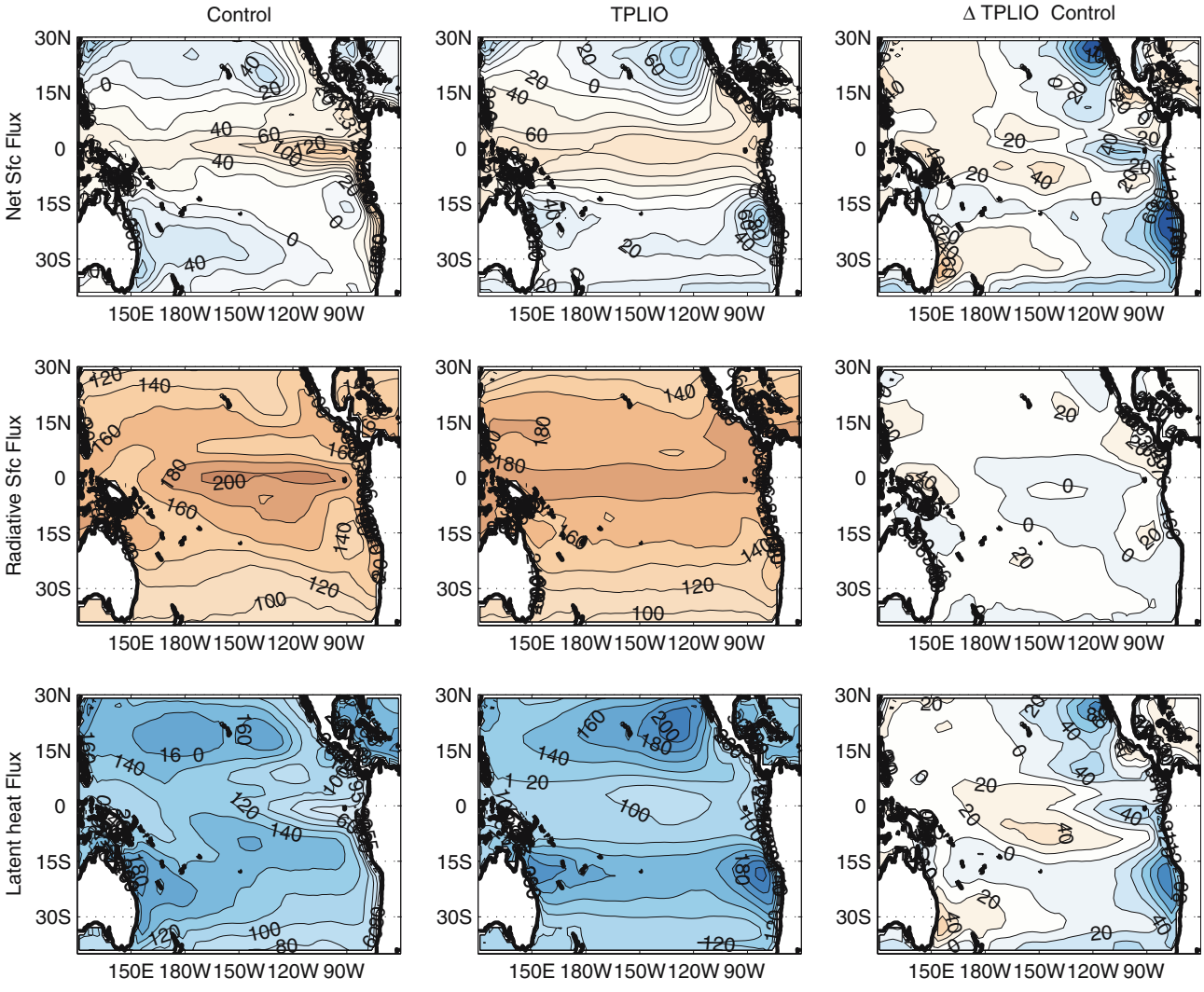

Fig. 9 Heat fluxes at the ocean surface for Control (*left column*), TPLIO (*middle column*) and the difference TPLIO–Control. Fluxes in W/m^2

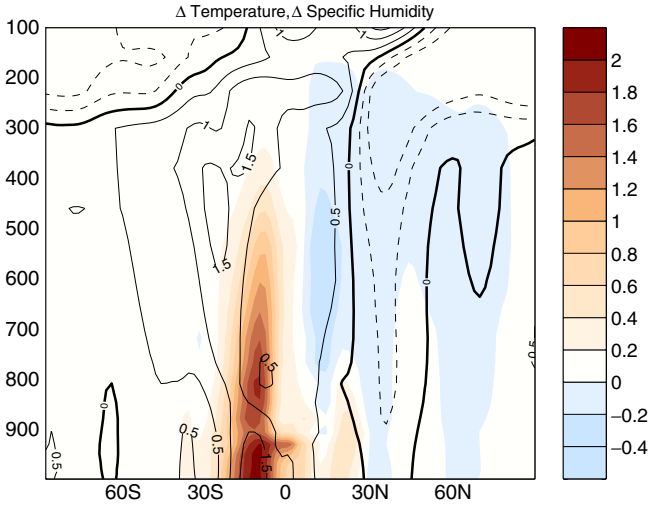

Fig. 10 Zonal annual mean difference of temperature and specific humidity (10e-3 g/kg, *color shading*) between TPLIO and Control

although annual global averages of fluxes at the top of the atmosphere and surface must be close to zero in an equilibrated coupled model, no such constraint applies when considering the atmosphere in isolation. Fluxes at the top and bottom of the atmosphere, jointly must then be in balance. If the atmosphere has below it an ocean with specified SST, then the ocean has infinite heat capacity.

Figure 10 shows the vertical structure of the warming of TPLIO with respect to Control. Between 60°S and 20°N, the atmosphere warming has a maximum of 1.5°C at about 400 mb. As we have seen above, the specific humidity in TPLIO with respect to Control increases significantly between 0 and 30°S because of the second ITCZ in the Pacific and the southward shift of the Atlantic ITCZ. In the northern tropics, a weaker ITCZ decreases the water vapor concentration. These changes are a consequence of cold regions becoming warm in TPLIO and sustaining

convection. The maximum warming is at upper levels where latent heat is released.

The Pliocene SST pattern also induces a global decrease in cloud cover, mainly because of a decrease in low-level clouds, especially in the tropics (Fig. 11, upper left panel). The zonal average of low-level cloud changes shows that they tend to decrease over the tropical band, with a minimum at the equator. High clouds (and to a lesser extent the mid-level clouds), on the other hand, decrease in the northern side of the equator and increase in the southern side in accord with the changes in convection described in Sect. 2.

The changes are small globally, but can be large locally. In the present-day tropics the low-level stratus clouds tend to occur in regions of high static stability, the subsidence regions of the Walker and Hadley circulations in the eastern sides of the oceans. Although the stratus clouds are not as pervasive as the high clouds (25 vs. 40% in the deep tropics), they shade the eastern basins from solar radiation contributing to the cool conditions there. The high cumulus clouds, on the other hand, tend to occur mainly in the western side of the basin and along the ITCZ where SSTs are relatively warm and wind convergence fuels convection. The demise of the Walker circulation and modifications in the Hadley cell in TPLIO change this picture. Since the regions of subsidence have shrunken, the stratus clouds diminish by about 50% and are replaced by high cumulus clouds signaling the presence of the double ITCZ (Fig. 11). There is also a reduction of high clouds in the western Pacific because of decreased convection. In the tropical Atlantic the southward shift of the ITCZ also reduces the stratus clouds.

Changes in the cloud distribution and type affect the radiation balance at the top of the atmosphere because different clouds have different optical properties. Since they are boundary layer clouds, low-level clouds cannot trap longwave radiation in the atmosphere. On the other hand, high-level clouds are very efficient in trapping longwave radiation because they radiate at temperatures characteristic of the cloud top which is colder than the Earth's surface. Consequently, the changes in outgoing longwave radiation between TPLIO and Control follow changes in the amount of high-level clouds with opposite sign (not shown). Both types of clouds, however, can reflect incoming shortwave radiation, and thus the variations in shortwave at the top of the atmosphere depends on total cloud changes. Nevertheless, changes in net radiation gain are controlled by changes in low-level clouds (Fig. 11, lower right panel). This is because changes in the longwave greenhouse effect and the shortwave albedo effect due to high-level cloud variations tend to cancel each other, a feature consistent with observations. As a result, the global mean radiative change at the top of the atmosphere for TPLIO is about 2.2 W/m^2, with an increase of 2.5 W/m^2 in incoming shortwave radiation and of 0.26 W/m^2 in outgoing longwave radiation. The net top of the atmosphere flux

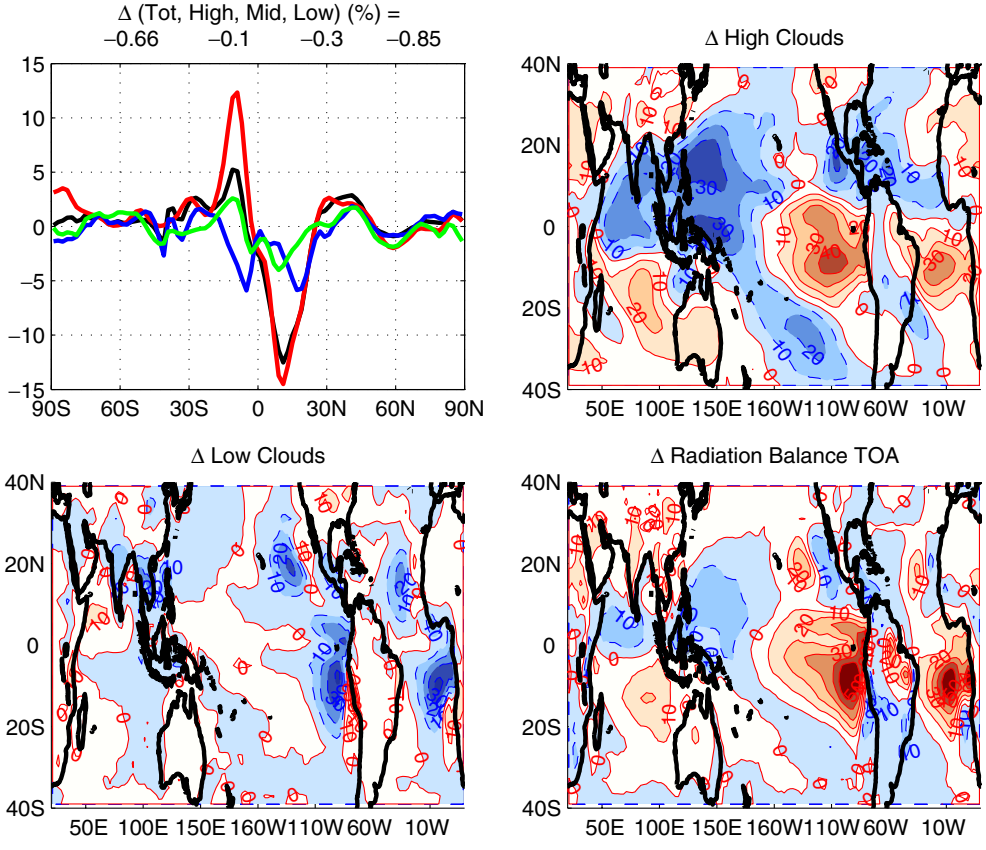

Fig. 11 **a** Annual zonal mean cloud amounts deviation TPLIO–Control (%): total (*black*), high (*red*), mid (*green*), low (*blue*). **b** Annual mean high-level cloud amount deviation TPLIO–Control (%). **c** Annual mean low-level cloud amount deviation TPLIO–Control (%). **d** Top of the atmosphere net radiative flux deviation between TPLIO and Control (W/m^2)

is balanced (to within 0.2 W/m^2 neglecting the work done by the atmosphere on the lower boundary) by an equal downward flux at the surface signaling that the atmosphere is in equilibrium. The changes in individual surface fluxes are as follows: a net downward shortwave increase of 1.9 W/m^2, a net downward longwave increase of 1.1 W/m^2, an increase in latent heat of 1.3 W/m^2, and a decrease in the sensible heat of 0.7 W/m^2.

We next compute the cloud radiative forcing (Ramanathan et al. 1989) as the difference between the clear sky and total sky radiative fluxes: $\mathrm{CRF} = \mathrm{CRF_{lw}} + \mathrm{CRF_{sw}} = (F_{\mathrm{clr}} - F) - (Q_{\mathrm{clr}} - Q)$, where F is the outgoing longwave radiation and Q is the absorbed solar radiation at the top of the atmosphere. Positive values of CRF have a heating effect on climate. Variations in CRF are not only contributed by clouds; variations of temperature and water vapor between clear- and cloudy-sky atmospheres can also influence CRF. This method, however, gives very similar results as other more elaborate procedures for calculating cloud feedbacks (Zhang et al. 1994). The variation in CRF between TPLIO and Control is Δ CRF = 1.8 W/m^2, which can be decomposed into $\Delta\ \mathrm{CRF_{lw}} = -0.5$ W/m^2 and $\Delta\ \mathrm{CRF_{sw}} =$ 2.3 W/m^2, which correspond to the long- and shortwave contributions, respectively. Thus, the changes in clouds described above provide a positive forcing on climate, and is mainly due to an increase in the absorbed shortwave radiation. According to our discussion this is due to the reduction of the low-level clouds consequence of the demise of the Walker circulation and modification of the Hadley cell.

4 Intermodel comparison

We use two other models to explore the sensitivity of the atmospheric response to a zero east–west tropical SST gradient: the NCAR model CAM3, and the Speedy GCM. The NCAR model is a state-of-the-art atmospheric GCM with horizontal resolution given by a spectral truncation T42 and has 26 vertical levels (Collins et al. 2004). The Speedy is an atmospheric GCM of intermediate complexity with low resolution (horizontal T30, eight vertical levels) and simplified physical parameterization schemes (Molteni 2003). As for AM2, each model is forced for 11 years with Control and TPLIO SST, and the differences between experiments over the last 4 years are analyzed. To compare with the AM2 we focus on atmospheric temperature, equatorial zonal wind stress, cloud changes and radiation at the top of the atmosphere.

Changes in the CAM3 model are similar to those in AM2. The absence of the equatorial east–west gradient increases the surface air temperature by 0.4°C and induces a double ITCZ in the tropical Pacific. The zonal mean vertical changes of temperature and specific humidity are very similar in magnitude and structure to those in AM2 (see Fig. 10). The Walker circulation collapses and the mean equatorial zonal wind stress vanish almost completely, while westerlies develop just south of the equator (Fig. 12). Compared to AM2, CAM3 presents weaker (almost zero) zonal mean equatorial wind stress when forced with TPLIO SST. This different response may be important to simulate a state of zero east–west gradient in a coupled model. The creation of a southern ITCZ induces changes in the tropical clouds so that the low-level clouds in the eastern Pacific are replaced by high-level clouds. Total cloud changes have similar structures as in AM2, and the reduction of planetary albedo increases the incoming solar radiation with magnitude and pattern comparables to that in AM2 (Fig. 13, upper panels).

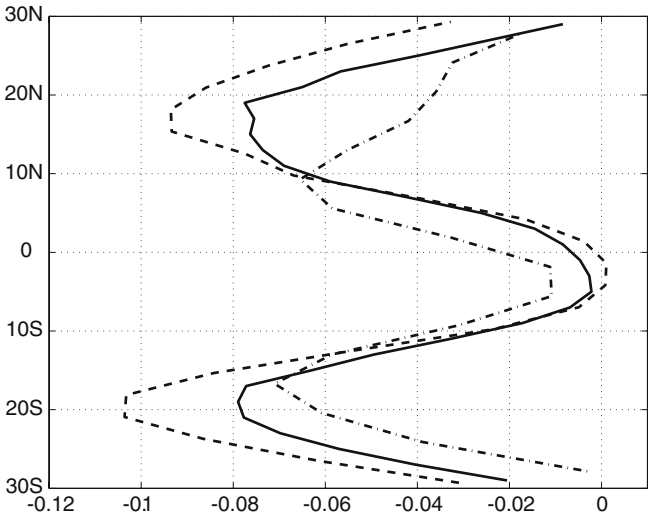

Fig. 12 Annual mean zonal wind stress in the tropical Pacific for TPLIO experiments in AM2 (*solid*), CAM3 (*dashed*) and Speedy (*dashed-dotted*)

Speedy warms up 0.6°C, but the atmospheric response is different than in AM2 and CAM3 models. The equatorial zonal wind stress diminishes with respect to Control, but healthy easterlies still prevail (Fig. 12). Larger differences occur in the top of the atmosphere radiation budget as a consequence of the fact that Speedy uses a much simpler parameterization of radiation processes than AM2 and CAM3 models. Most important is that Speedy has only one type of clouds, and therefore it cannot differentiate between the radiation properties of different cloud types. In this model, the ITCZ in the tropical Pacific shifts south of the equator, decreasing the cloudiness to the north and increasing it to the south of the equator (Fig. 13, lower left panel). This is similar to the total cloud changes seen in AM2 (or CAM3), which have a similar structure as changes in high clouds (not shown, see Fig. 11). However, contrary to the AM2, there is decreased incoming shortwave radiation in the region of stratus clouds because in Speedy the albedo is proportional to the cloud amount which increases in these regions. As a consequence, contrary to AM2 and CAM3 models, Speedy has a net flux loss at the top of the atmosphere in TPLIO

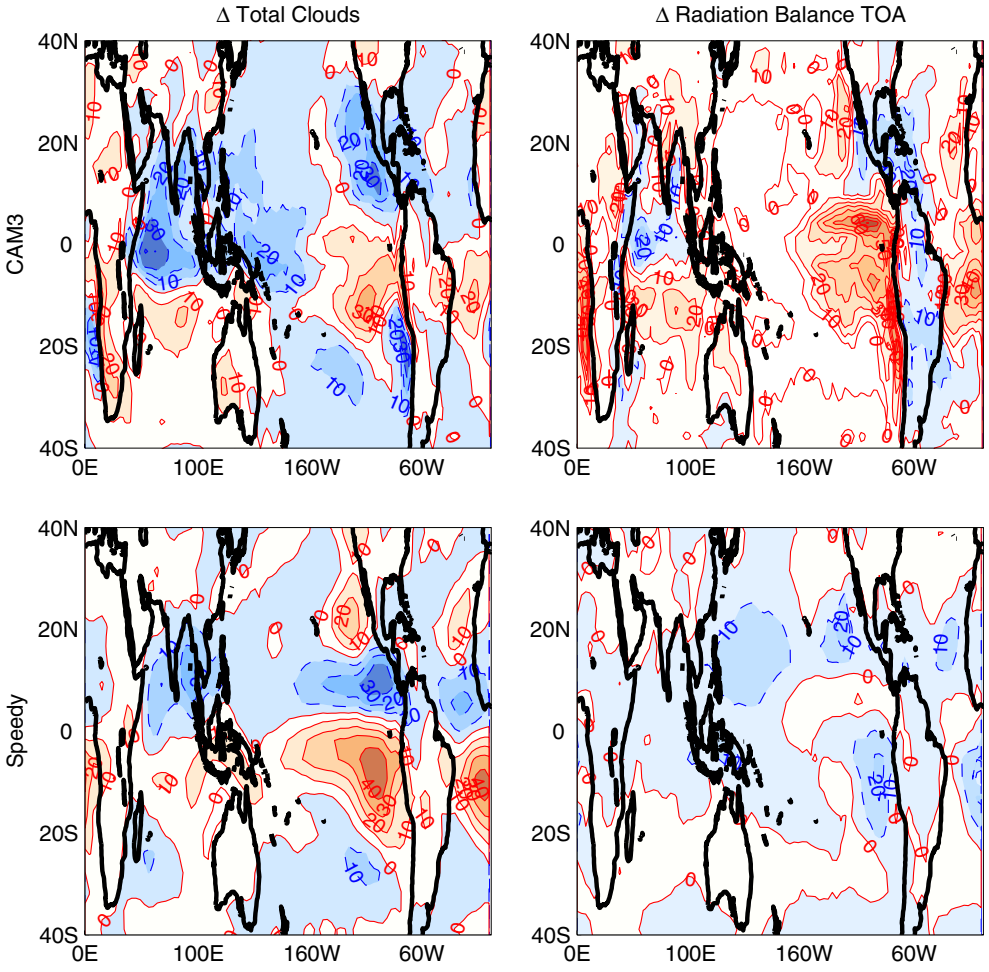

Fig. 13 Changes in total cloud amount and top of the atmosphere radiation balance for TPLIO experiment with respect to Control in CAM3 (*upper panels*) and Speedy (*lower panels*)

with respect to Control (1.4 W/m^2, Fig. 13, lower right panel). The tropical atmospheric warming is similar to that in AM2, but with a maximum of 2.0°C that occurs on the equator at higher levels (300 mb).

This intermodel comparison points out the difficulty in representing cloud–radiation interactions and stresses the need to use complex representations of these processes to get a satisfactory answer.

5 Sensitivity to SST forcing

This section explores the sensitivity of the atmospheric response to other SST forcings using the AM2 model. To do so we constructed the following SST (12-month) data sets:

- TPLIO1K: the conditions are the same as for TPLIO except that between 40°S and 30°N SSTs are increased by 1 K.
- TPLIO_noice: the conditions are the same as for TPLIO but ice is removed from the NH, on land and sea. Over land the ice-covered regions are replaced with tundra, while in the newly open areas of water SST is set at 0°C. The topography over Greenland is decreased to 1/4 of its present value, which roughly takes into account the removal of the ice and the continental rebound (Bamber et al. 2001).
- UNIF2K: in this simulation the seasonal cycle of SST is that of today, except for a uniform increase of 1.9°C between 40°S and 30°N. Specified ice on land and sea correspond to conditions of today. The global change of SST with respect to today's global mean is the same as in TPLIO1K.

All data sets are blended by a linear interpolation from the modified tropical SST to the present-day extratropical SST.

Wara et al. (2005) point out that while the east–west gradient was absent during the early Pliocene, the calibration of the data results in a range of absolute temperature estimates. Thus, TPLIO and TPLIO1K test the sensitivity of the AM2 to the absolute value of tropical SST, and provide a range for the contribution of tropical conditions to Pliocene warmth. On the other hand, TPLIO_noice and TPLIO evaluate the relative importance of tropical SSTs and the northern ice cap in the climate of 3 Ma. Finally, UNIF2K and TPLIO1K provide the insight into the sensitivity of the atmospheric response to two different warming SST patterns in the

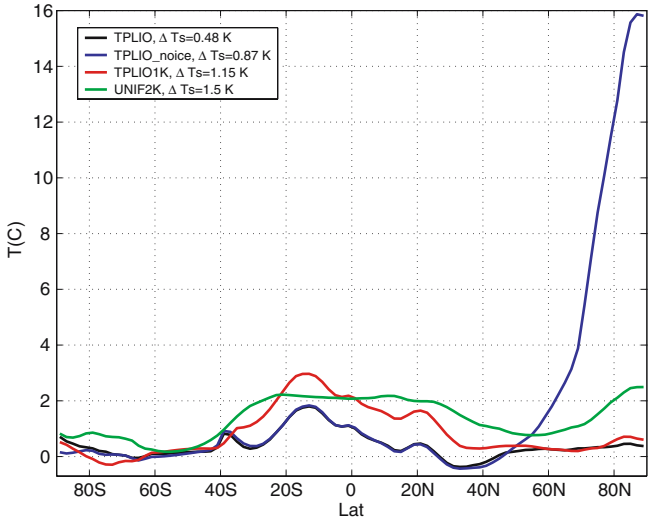

Fig. 14 Annual zonal mean surface air temperature deviations from Control for different experiments

tropics. A warming of the type used in UNIF2K, but over the global oceans, has been used as a surrogate of climate change for comparing climate feedback processes in atmospheric GCMs (Cess et al. 1990; Soden et al. 2004).

Figure 14 shows the zonally averaged annual mean surface air temperature deviation of each experiment relative to the Control run. As mentioned before, in TPLIO the mean global surface air temperature increases by about 0.5°C. The increase is larger (1.15°C) when the SST is increased uniformly by 1°C (TPLIO1K). The warming is mainly in the tropics. As in the TPLIO case, the low-level cloud changes dominate the radiation balance at the top of the atmosphere. More solar radiation enters the atmosphere (1.6 W/m^2) but this is offset by increased emission of longwave radiation into space (1.0 W/m^2) due to significantly more water vapor content in the atmosphere.

When the ice coverage in the NH is removed, the northern pole shows a huge surface warming of about 16°C. The response is largest in winter due to the release of heat from the now ice-free Arctic Ocean. This warming is, however, confined to a very small region of the globe (north of 50°N), in agreement with previous studies (e.g., Crowley et al. 1994).

The UNIF2K experiment shows a global mean warming of 1.5°C. Compared to TPLIO1K, the largest differences are in the NH extratropics because the atmospheric anomalies in UNIF2K tend to warm the NH extratropics more efficiently than in TPLIO1K, particularly in the boreal winter (see also next section). Figure 15 shows the spatial pattern of temperature changes during December–February together with the accompanying sea-level pressure anomaly. The circulation anomalies induced in UNIF2K are displaced with respect to those in TPLIO1K so that they tend to be stronger over the continents, thus warming the surface by temperature and moisture advection. The major difference in the warming pattern occurs in the NH Polar regions where UNIF2K shows a warming in excess of 2°C, while TPLIO1K shows almost no anomaly. The importance of the tropical SST patterns for the extratropical climate is readily seen.

5.1 Comparison of TPLIO with UNIF2K

It is instructive to compare in further detail the atmospheric response in the TPLIO experiment with that in UNIF2K in which the present-day east–west SST gradient is preserved, but the tropical SSTs are uniformly increased by 1.9°C. As result of the different forcing, the adjustment of the tropical atmosphere in UNIF2K is quite different from that in TPLIO.

The tropical atmospheric circulation in UNIF2K has similar structure to present-day circulation, with a healthy Walker cell and no significant changes in the Hadley cell (not shown). There is no net change in global total cloud amount between UNIF2K and Control. Global low-level cloud amounts increase slightly by 0.3%, while the total and high-level cloud amounts remain unchanged.

A sensitivity experiment in which the tropical SSTs were increased uniformly by 5°C also show minor changes in low-level clouds. This result can be understood by following the discussion in Miller (1997) who argues that low-level static stability of the atmosphere in the eastern oceans is not only given by the local SST but by the difference between potential temperature at 700 mb and SST, that is $\Delta\theta_e = \theta(700\ mb) - \mathrm{SST}_e$. In the tropics the large-scale circulation maintains a nearly uniform horizontal distribution of temperature above the inversion. Furthermore, convection in the western oceans, through a moist-adiabatic, relates the vertical temperature profile to the local SST. Therefore, potential temperature above the trade inversion varies with the SST in the western ocean, and the low-level static stability in the cold tongue region can be written as $\Delta\theta_e = \Delta\theta_w + (\mathrm{SST}_w - \mathrm{SST}_e)$. Parameter $\Delta\theta_w$ is a measure of the low-level static stability in the west and is equal to the increase in θ between the surface and 700 mb. According to that equation the east–west gradient of SST controls the static stability of the eastern oceans. As long as $(\mathrm{SST}_w - \mathrm{SST}_e) > 0$, $\Delta\theta_e > \Delta\theta_w$ and the low-level stratus clouds will persist because the eastern ocean will be the region of subsidence.

The similarity between UNIF2K and Control can be seen in the difference in annual zonal mean of freshwater flux. Since there are no major reorganizations of the tropical circulation, the precipitation patterns are similar to the present. The only difference is a stronger (5%) hydrological cycle: it rains more in the tropics, less in subtropics and more in high latitudes (Fig. 6, lower panel). Note that changes in freshwater flux into the ocean are much smaller in UNIF2K than in TPLIO.

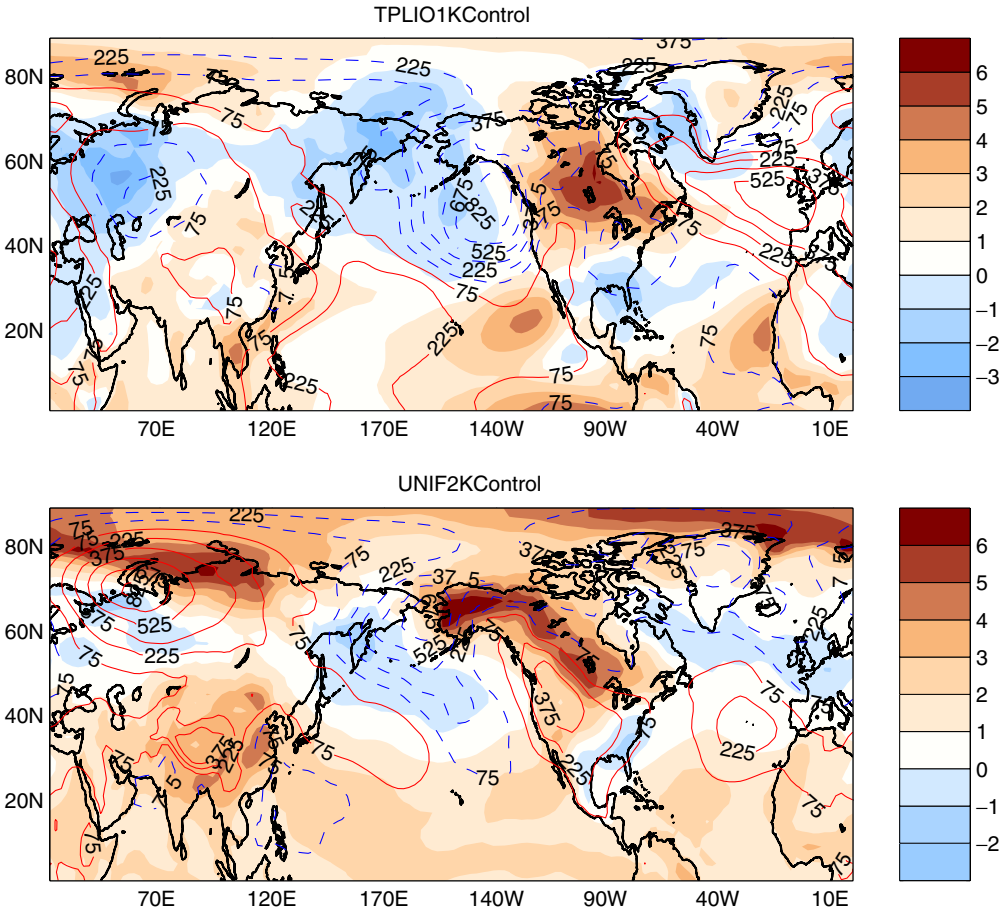

Fig. 15 Deviations of surface air temperature (C, *color shading*) and surface pressure (Pa) with respect to Control during DJF for TPLIO1K (*upper panel*) and UNIF2K (*lower panel*)

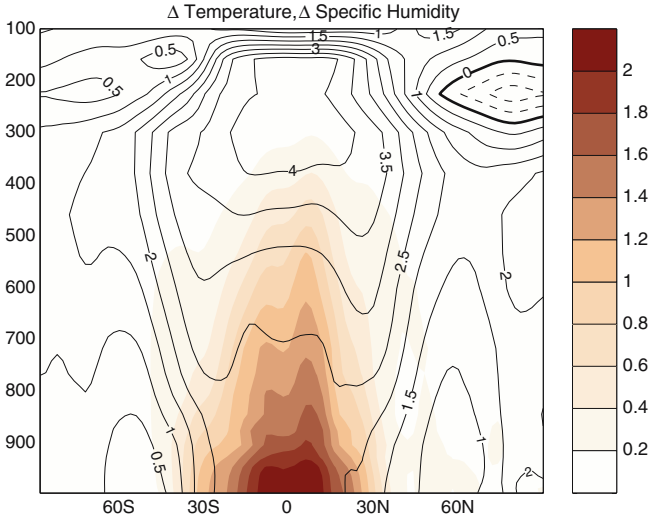

Fig. 16 Zonal annual mean difference of specific humidity (10e-3 g/kg, *color shading*) and temperature between UNIF2K and Control

In UNIF2K the tropical adjustment to the new SST can be interpreted as the result of the atmospheric tendency to follow a warmer moist-adiabatic without significantly changing the clouds. This in turn dictates the radiative and latent heat fluxes. Figure 16 shows the variation of specific humidity of UNIF2K with respect to Control. Water vapor increases everywhere, and it is largest at the lower levels and at latitudes where upward motion dominates. The increase in water vapor in this experiment is much larger than in TPLIO. The tropospheric temperature change in the tropical region shows a stronger warming in the upper than at lower levels due to the release of latent heat. This change in the thermal structure, or lapse rate, acts as a negative feedback because it leads to more emission of longwave radiation to space. The above patterns of temperature and humidity changes are very similar to those reported by other authors in surrogates of climate change (Cess et al. 1990).

This discussion can be further quantified by calculating the top of the atmosphere fluxes. As expected, changes in outgoing longwave radiation dominate the balance at the top of the atmosphere: UNIF2K loses 2.6 W/m^2 more longwave radiation than Control, and also absorbs less solar radiation (1.0 W/m^2) than Control. The increase in outgoing longwave radiation and atmospheric warming is mainly a clear-sky process. The small cloud changes tend to provide a negative forcing on climate (Δ CRF $= -0.8$ W/m^2). On the other hand,

the flux changes at the surface are: equal decreases in the incoming shortwave and upward longwave of 2.7 W/m^2, an increase in latent heat of 3.9 W/m^2, and a small reduction in sensible heat of 0.1 W/m^2. Thus, the main adjustment process involves a reduction in the lapse rate and increased atmospheric water vapor which lead to more (longwave) radiative cooling, and in turn is mainly balanced by increased latent heat release from condensation. This balance was confirmed by performing a heat budget analysis as in Knutson and Manabe (1995). Moreover, this has been shown to be the primary energy balance in the tropics (Pierrehumbert 1995), and the mechanism through which the atmosphere warms during El Niño events (Soden 2000). The increased surface evaporation maintains the stronger hydrological cycle mentioned above.

In UNIF2K the atmospheric relative humidity stays constant. This implies that the water vapor content of each atmospheric layer increases with temperature according to the Clausius–Clapeyron relation. Previous experiments with atmospheric GCMs predict that the relative humidity distribution is largely insensitive to changes in climate (Held and Soden 2000). The constraint of fixed relative humidity is maintained better at lower levels because air aloft is highly unsaturated. Interestingly, TPLIO and TPLIO1K have larger global mean relative humidity than Control throughout the troposphere. The deviation is about 1% up to 400 mb, but locally can exceed 10% as a result of the reorganization of tropical convection that changes the Walker and Hadley cells and thus the upward transport of moisture.

It is important to note that while in UNIF2K the net flux at the top of the atmosphere (and at the surface) is upward, in TPLIO the net flux is downward. The upward flux in UNIF2K is mainly due to the increased outgoing longwave radiation to space, and acts as a negative feedback to the imposed warmer SST. In TPLIO, the net downward flux is mainly a consequence of the changes in the clouds that change the Earth's albedo and allow more incoming solar radiation. Since the atmosphere is relatively transparent to shortwave only a minor fraction of it is absorbed on its way down by water vapor and clouds. The rest of the extra solar radiation reaches the surface where it plays no role because SSTs are imposed (except over land). Thus, the effect of changes in the Earth's albedo are not fully realized in TPLIO because SST are imposed, and the increase in surface temperature described above can be considered as a lower bound.

We can estimate the first-order effect of the radiative imbalance at the top of the atmosphere in the Earth's climate using the climate sensitivity of the model. We calculate the climate sensitivity using experiment UNIF2K, which is similar to the experiments used to estimate this quantity in the literature (e.g., Cess et al. 1990). The surface air temperature increase in UNIF2K is 1.5°C and there is a net loss of 3.6 W/m^2 at the top of the atmosphere with respect to Control, resulting in a climate sensitivity of $\lambda = 0.42°\ C/\mathrm{W/m^2}$. Thus, the 2.2 W/m^2 imbalance at the top of the atmosphere in TPLIO would result in a surface warming of 0.9°C if the ocean–atmosphere system were allowed to equilibrate while maintaining the same tropical SST pattern. This additional warming due to a decrease in the Earth's albedo adds to the previously mentioned increase in surface air temperature of 0.5°C in TPLIO. Consequently, the absence of the cold tongue would have warmed the Pliocene climate by about 1.4°C. In this equilibration process the SST would increase together with the atmospheric temperature. Assume, as a simplification, that during the equilibration process mainly the tropical SST would increase, and that they do so uniformly. Then, the pattern would be similar to that of experiment TPLIO1K. In this experiment the net downward flux at the top of the atmosphere is 0.6 W/m^2 (significantly smaller than in TPLIO experiment), which using the climate sensitivity λ implies a further warming of 0.25°C. Thus, the implied total increase in surface air temperature is 1.4°C, the same as the value implied in TPLIO. This result gives confidence in the estimation of a total increase in global surface temperature of 1.4°C due to the absence of the upwelling regions. This is merely a first-order estimate. Experiments with a coupled model are needed to further investigate the effect of these albedo changes in the Pliocene climate.

6 Summary and discussion

Several authors (e.g., Sloan et al. 1996; Haywood et al. 2000) have simulated Pliocene climates imposing the PRISM data sets as boundary conditions to atmospheric GCMs. Particularly important in these experiments is the SST data, which deviate from present values mainly in the high latitudes; in the tropics there is little change from today's values. Those results indicate a Pliocene warming of 1.9–3.6°C with respect to the present climate.

In agreement with PRISM2, other recent paleo-data suggest that western tropical Pacific SST during the early Pliocene were similar to today's. However, in the eastern Pacific where the PRISM2 reconstruction has limited coverage, the non-PRISM data suggest the absence of cold surface waters at that time (Wara et al. 2005; Haywood et al. 2005). Surface temperatures in the upwelling regions of the Atlantic ocean were similarly high (e.g., Marlow et al. 2000). We investigate the atmospheric circulation consistent with such a zonally uniform state of no east–west SST gradient in the tropical oceans, and explore whether the tropical conditions could have contributed to the warmer climate experienced during the mid-Pliocene. In the model, the atmospheric conditions include a double ITCZ with very weak equatorial trades and a collapsed Walker circulation. The low-level tropical stratus clouds diminish greatly, reducing the albedo of the Earth and allowing more incoming solar radiation. The tropical atmosphere warms up between 0.5 and 1.5°C, with a maximum at

higher levels, due to the release of latent heat accompanying the increased evaporation. In the extratropics, changes in the circulation through atmospheric teleconnection mechanisms originating in the tropical Pacific induce a substantial warming over North America, which is further enhanced by surface albedo feedbacks. This process may have contributed to a ice-free North America during the Pliocene. All these mechanisms warm the surface air temperature between 0.5 and 1.4°C when the effects of changes in the Earth's albedo are estimated using the model's climate sensitivity. The sensitivity of the atmospheric adjustment to mid-Pliocene tropical conditions was assessed by forcing different models with TPLIO SSTs. Results are dependent on the physical parameterizations of the models, particularly the cloud-radiation processes, which are a major source of uncertainty in current climate models. Nevertheless, the two state-of-the-art atmospheric GCMs used here tend to agree quite well. Previous authors have suggested several hypotheses to explain the Pliocene warmth. These include increased atmospheric CO_2, cryospheric changes and a strong thermohaline circulation. The closing of the Panama seaway has also been connected to the onset of the NH glaciation and the end of the Pliocene warm climate (Haug and Tiedemann 1998). Our results do not directly contradict any of these hypotheses but instead advance another mechanism, namely the changes in the tropical atmospheric circulation due to the absence of the east–west SST gradient that characterizes the present equatorial ocean. We have shown that the tropical SST pattern during the Pliocene is very important for extratropical latitudes so that a complete understanding of Pliocene climate depends critically on determining the tropical conditions at that time, as pointed out by Crowley (1996).

In this study we have used an atmospheric GCM to determine the atmospheric circulation consistent with the absence of the east–west SST gradient that characterizes today's tropical oceans. The next step is to find the ocean state consistent with the atmospheric fluxes of momentum, freshwater and heat obtained from this experiment. Can those fluxes maintain the absence of tropical east–west SST gradient? Can this state be maintained in a fully coupled model? These questions are addressed in a separate paper.

Acknowledgements This research is supported in part by NASA Grant NAG5-12387 and NOAA Grant NA16GP2246. We thank Isaac Held, Syukuro Manabe, Venkatachalam Ramaswamy, Christina Ravelo and Brian Soden for useful discussions, and Cathryn Meyer for helping with NCAR CAM calculations at Yale University. We also thank the reviewers for their constructive comments.

References

Bamber JL, Layberry RL, Goginemi SP (2001) A new ice thickness and bed data set for the Greenland ice sheet 1 measurement, data reduction, and errors. J Geophys Res 106(D24):33773–33780

van der Burgh J, Visscher H, Dilcher DL, Kürschner WM (1993) Paleoatmospheric signatures in fossil leaves. Science 260:1788–1790

Cannariato KG, Ravelo AC (1997) Pliocene–Pleistoce evolution of eastern tropical Pacific surface water circulation and thermocline depth. Paleoceanography 12(6):805–820

Cess RD et al (1990) Intercomparison and interpretation of climate feedback processes in 19 atmospheric general-circulation models. J Geophys Res 95:16601–16615

Chaisson WP, Ravelo AC (2000) Pliocene development of the east-west hydrographic gradient in the equatorial Pacific. Paleoceanography 15:497–505

Collins WD et al (2004) Description of the NCAR Community Atmospheric Model (CAM3). Technical Report NCAR/TN-464 + STR, National Center for Atmospheric Research, Boulder, Colorado 80307-3000, 226pp

Crowley TJ (1996) Pliocene climates: the nature of the problem. Mar Micropaleontol 27:3–12

Crowley TJ, Yip K-J, Baum SK (1994) Effect of altered Arctic sea ice and Greenland ice sheet cover on the climate of the GENESIS general circulation model. Global Planet Change 9:275–288

Dowsett H, Barron J, Poore R (1996) Middle Pliocene sea surface temperatures: a global reconstruction. Mar Micropaleontol 27:13–25

Dowsett HJ, Barron JA, Poore RZ, Thompson RS, Cronin TM, Ishman SE, Willard DA (1999) Middle Pliocene paleoenvironmental reconstruction: PRISM2. USGS Open File Report 99-535, http://pubs.usgs.gov/openfile/of99-535

Dowsett HJ, Chandler MA, Cornin TM, Dwyer GS (2005) Middle Pliocene sea surface temperature variability. Paleoceanography 20, doi:10.1029/2005PA001133

GDFL Global Atmospheric Model Development Team (2005) The new GFDL global atmosphere and land model AM2/LM2: Evaluation with prescribed SST simulations. J Climate (in press)

Haug HH, Tiedemann R (1998) Effect of the formation of the Isthmus of Panama on Atlantic Ocean thermohaline circulation. Nature 393:673–676

Haywood AM, Valdes PJ (2004) Modelling Pliocene warmth: contribution of atmosphere, oceans and cryosphere. Earth Planet Sci Lett 218:363–377

Haywood AM, Valdes PJ, Sellwood BW (2000) Global scale palaeoclimate reconstruction of the middle Pliocene climate using the UKMO GCM: initial results. Global Planet Change 25:239–256

Haywood AM, Dekens P, Ravelo AC, Williams M (2005) Warmer tropics during the mid-Pliocene? Evidence from alkenone paleothermometry and a fully coupled ocean-atmosphere GCM. Geochem Geophys Geosys 6, doi:10.1029/2004GC000799

Held IM, Soden BJ (2000) Water vapor feedback and global warming. Annu Rev Energy Environ 25:441–475

Herbert TD, Shuffert JD (1998) Alkenone unsaturation estimates of late Miocene through late Pliocene sea-surface temperature at site 958. In: Proceedings of the Ocean Drilling Program, pp17–21

Hess PG, Battisti DS, Rasch JR (1993) Maintenance of the intertropical convergence zones and the large-scale tropical circulation on a water-covered earth. J Atmos Sci 50:691–713

Kim SJ, Crowley TJ (2000) Increased Pliocene North Atlantic deep water: cause or consequence of Pliocene warming? Paleoceanography 15(4):451–455

Knutson TR, Manabe S (1995) Time-mean response over the tropical Pacific to increased CO_2 in a coupled ocean-atmosphere model. J Climate 8:2181–2199

Marlow JR, Lange CB, Wefer G, Rosell-Melé A (2000) Upwelling intensification as part of the Pliocene-Pleistocene climate transition. Science 290:2288–2291

Miller RL (1997) Tropical thermostats and low cloud cover. J Climate 10:409–440

Molnar P, Cane MA (2002) El Niño's tropical climate and teleconnections as a blueprint for pre-Ice Age climates. Paleoceanography 17(2), doi:10.1029/2001PA000663

Molteni F (2003) Atmospheric simulations using a GCM with simplified physical parametrizations I: model climatology and variability in multi-decadal experiments. Clim Dynam 20:175–191

Philander SG, Fedorov AV (2003) Role of tropics in changing the response to Milankovich forcing some three million years ago. Paleoceanography 18(2), doi:10.1029/2002PA000837

Pierrehumbert RT (1995) Thermostat, radiator fins and the local runaway greenhouse effect. J Atmos Sci 152:1784–1806

Ramanathan V, Cess RD, Harrison EF, Minnis P, Barkstrom BR, Ahmad E, Hartmann D (1989) Cloud-radiative forcing and climate: results from the Earth Radiation Budget experiment. Science 243:57–63

Ravelo AC, Andreasen DH (2000) Enhanced circulation during a warm period. Geophys Res Lett 27:1001–1004

Ravelo AC, Andreasen DH, Lyle M, Olivarez Lyle A, Wara M (2004) Regional climate shifts caused by gradual global cooling in the Pliocene epoch. Nature 429:263–267

Raymo ME, Grant B, Horowitz M, Rau GH (1996) Mid-Pliocene warmth: Stronger greenhouse and stronger conveyor. Mar Micropaleontol 27:313–326

Rickaby REM, Halloran P (2005) Cool La Niña during the warmth of the Pliocene? Science 307:1948–1952

Sloan LC, Crowley TJ, Pollard D (1996) Modeling of middle Pliocene climate with the NCAR GENESIS general circulation model. Mar Micropaleontol 27:51–61

Soden BJ (2000) The sensitivity of the tropical hydrologic cycle to ENSO. J Climate 13:538–549

Soden BJ, Broccoli AJ, Hemler RS (2004) On the use of cloud forcing to estimate cloud feedback. J Climate 17:3661–3665

Thompson RS, Fleming RF (1996) Middle Pliocene vegetation: reconstructions, paleoclimatic inferences, and boundary conditions for climate modeling. Mar Micropaleontol 27:27–49

Wara M, Ravelo AC, Delaney ML (2005) Permanent El Niño conditions during the Pliocene warm period. Science 309:758–761

Yin JH, Battisti DS (2001) The importance of tropical sea surface temperature patterns in simulations of Last Glacial Maximum climate. J Climate 14:565–581

Zachos J, Pagani M, Sloan L, Thomas E, Billups K (2001) Trends, rhythms, and aberrations in global climate 65 Ma to present. Science 292:686–693

Zhang MH, Cess RD, Hack JJ, Kiehl JT (1994) Diagnostic study of climate feedback processes in atmospheric GCMs. J Geophys Res 99:5525–5537